**Supplementary Information**

# Hybrid 1D/2D nanocarbon-based conducting polymer nanocomposites for high-performance wearable electrodes

Dong Young Kim,*[a] † Geonhee Lee,[b]† Gil Yong Lee,[b] Jungpil Kim,[c] Kwangu Jeon[d], and Keun Soo Kim*[b]

[a] Convergence Research Division, Korea Carbon Industry Promotion Agency (KCARBON), 111, Biseongnal-ro, Deokjin-gu, Jeonju-si, 54852 Korea.

[b] Department of Physics, Graphene Research Institute, and GRI-TPC International Research Centre, Sejong University, Seoul 05006, Republic of Korea.

[c] Carbon Materials Application Research Group, Korea Institute of Industrial Technology (KITECH), 222 Palbok-ro, Deokjin-gu, Jeonju 54853, Republic of Korea

[d] E-Cube Materials, Palbok-dong, Deokjin-gu, Jeonju-si, Jeollabuk-do, Republic of Korea

† These authors contributed equally.

* Corresponding authors.

*E-mail addresses*: dykim@kcarbon.or.kr (D. Y. Kim), kskim2676@sejong.ac.kr (K. S. Kim)

**Table S1.** Parameters of the fabricated conducting nanocomposite film.

| Materials | | Ratio of materials in PDMS (SWCNTs / r-GO) | Curing conditions | |
|---|---|---|---|---|
| | | | Temp. (℃) | Time (h) |
| Fabricated nanocomposite conducting film | PDMS-r-GO | 0 : 2 | 130 | 2 |

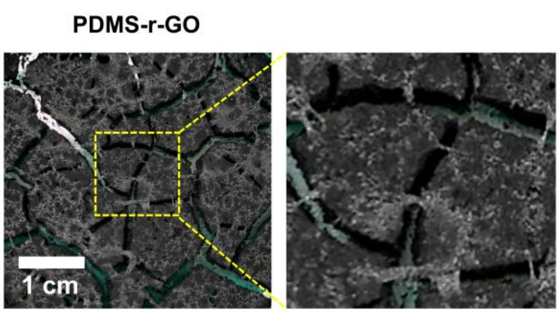


**Fig. S1** Digital photographs of the PDMS-r-GO sample. The nanocomposite film based on PDMS-r-GO (2 wt.%) shows a small broken structure despite the equal fabrication process.

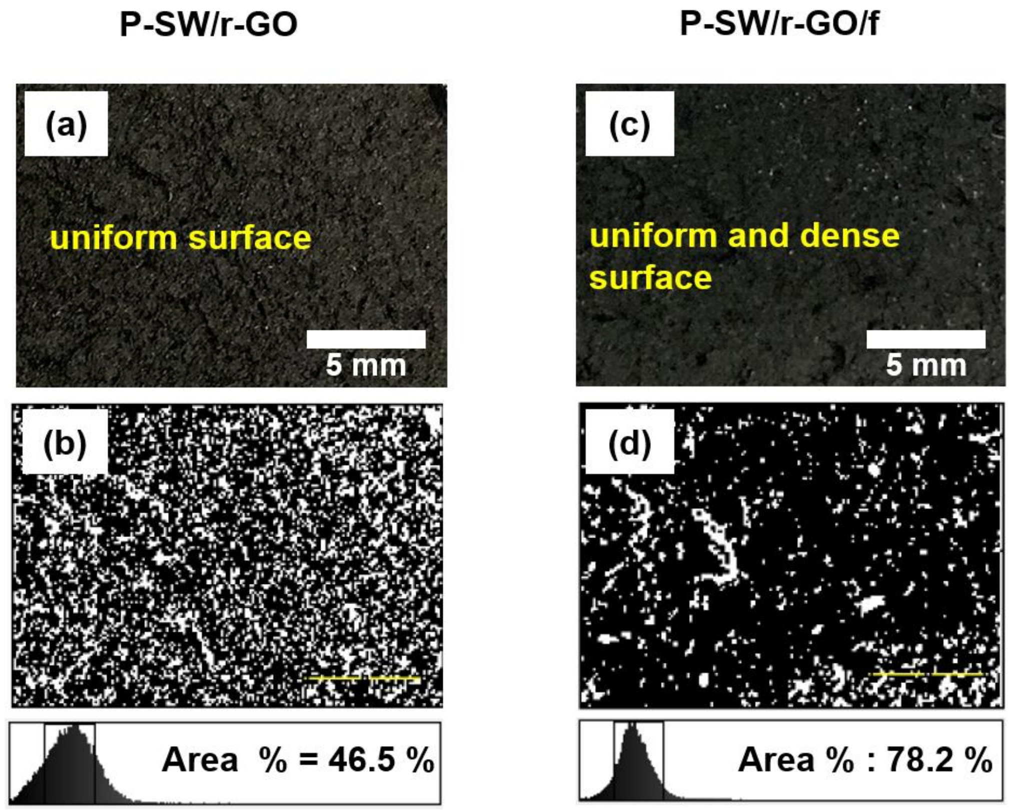


**Fig. S2** Area fraction measurement of darkness on surface of P-SW/r-GO and P-SW/r-GO/f samples using ImageJ analysis. (a) digital photograph and (b) ImageJ of the P-SW/r-GO. (c) digital photograph and (d) ImageJ of the P-SW/r-GO/f. Area fraction values of P-SW/r-GO and P-SW/r-GO/f are indicated 46.5 and 78.2 %, respectively.

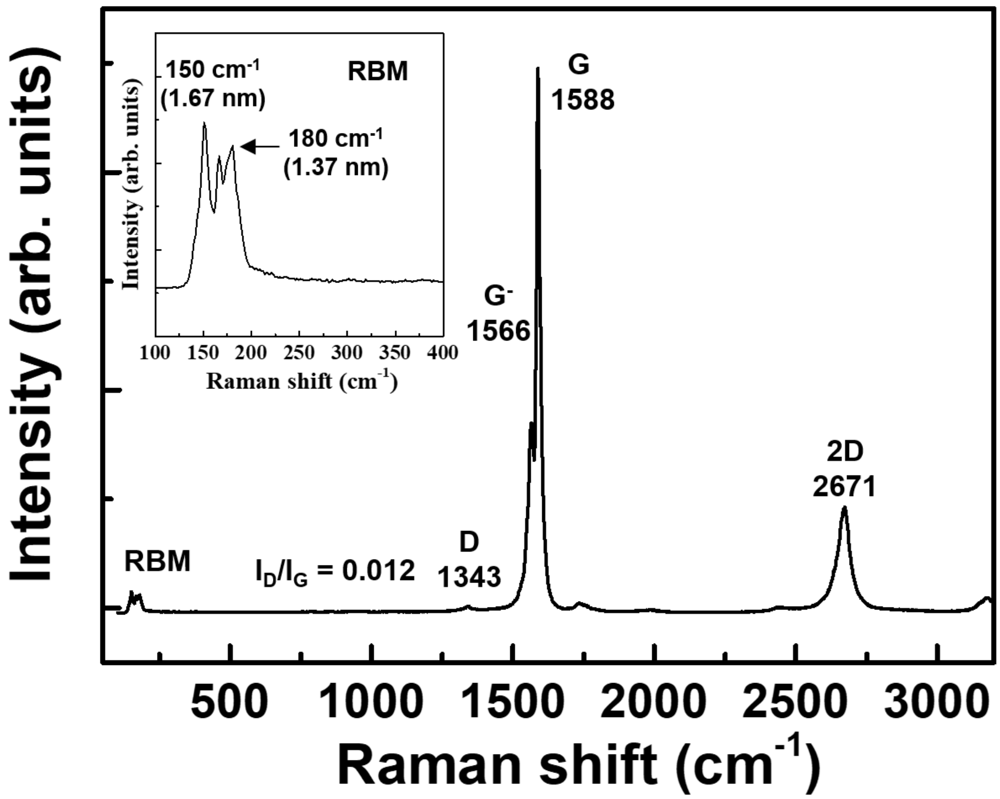


**Fig. S3** Raman spectra of the pristine SWCNTs. The inset shows RBM region of the SWCNTs.

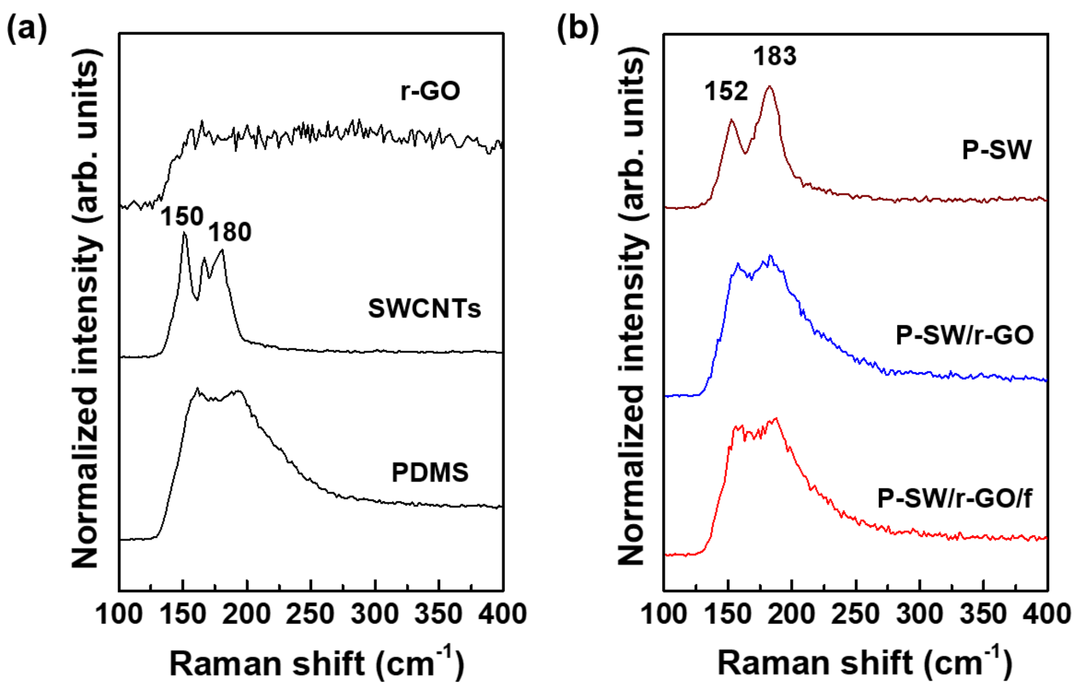


**Fig. S4** Raman spectra in RBM region. (a) PDMS, SWCNTs, and r-GO as raw samples. (b) P-SW, P-SW/r-GO and P-SW/r-GO/f as conducting nanocomposite films.

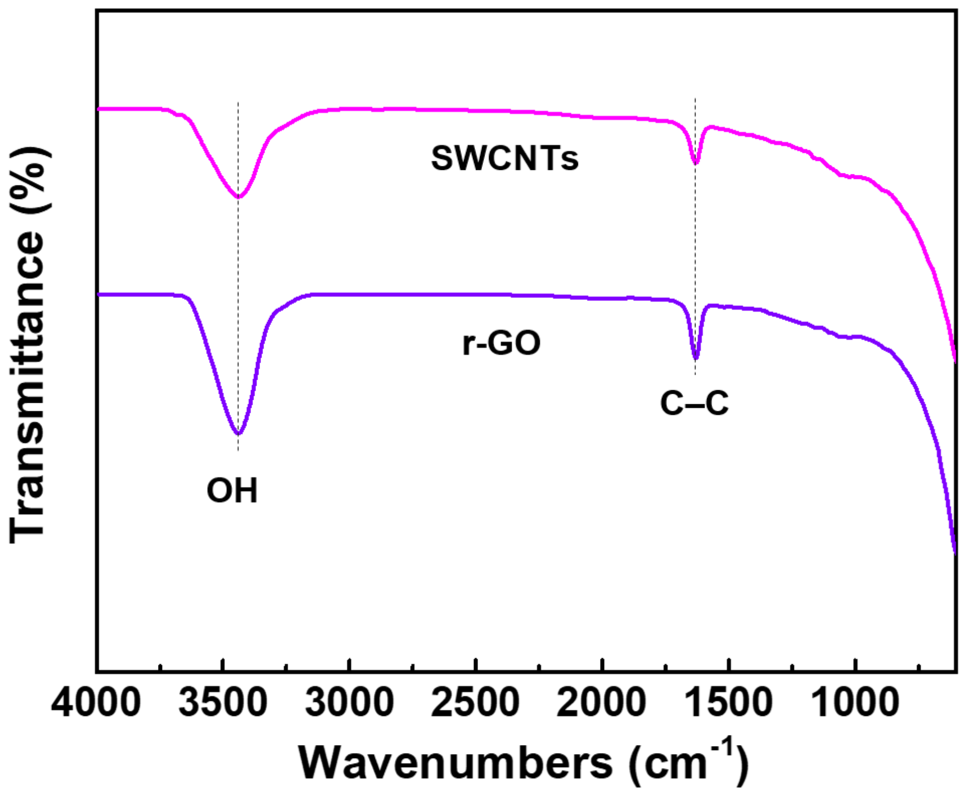


**Fig. S5** FTIR spectra of pristine SWCNTs and r-GO samples.

**Table S2.** XPS elemental analysis results for pristine and nanocomposite samples.

| Materials | | Element (at.%) | | | |
|---|---|---|---|---|---|
| | | C | O | Si | Total |
| Pristine samples | PDMS | 49.3 | 24.0 | 26.7 | 100 |
| | SWCNTs | 96.0 | 2.8 | 1.2 | 100 |
| | r-GO | 93.1 | 5.1 | 0.6 | 100 |
| Fabricated nanocomposite conducting films | P-SW | 48.8 | 24.3 | 26.9 | 100 |
| | P-SW/r-GO | 51.3 | 22.9 | 25.8 | 100 |
| | P-SW/r-GO/f | 46.4 | 26.5 | 27.1 | 100 |

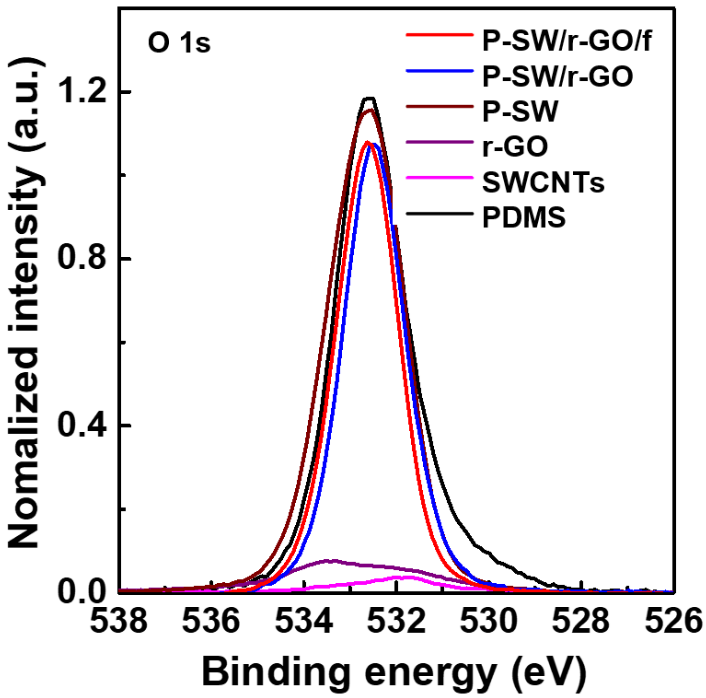


**Fig. S6** O 1s XPS spectra of the PDMS, SWCNTs, r-GO, and conducting nanocomposite films.

**Table S3**. FWHMs of C 1s spectra for pristine and nanocomposite samples.

| Samples | FWHMs form C 1s spectra (eV) |
|---|---|
| PDMS | 1.722 |
| SWCNTs | 0.954 |
| r-GO | 1.181 |
| P-SW | 1.720 |
| P-SW/r-GO | 1.455 |
| P-SW/r-GO/f | 1.491 |

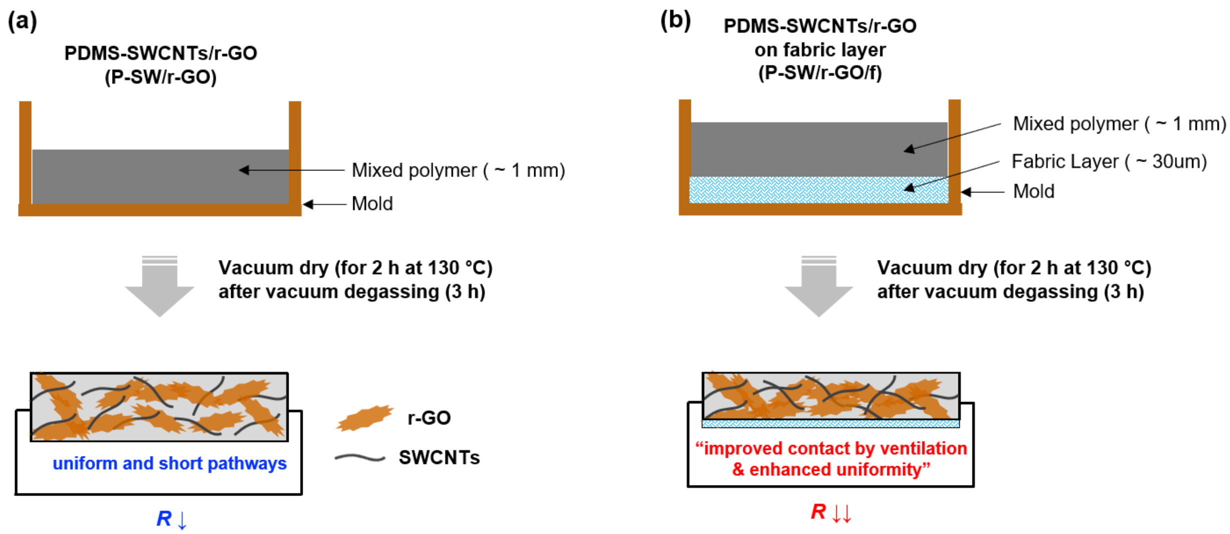


**Fig. S7** Schematic of the fabricated conductive nanocomposite electrode for the (a) P-SW/r-GO and (b) P-SW/r-GO/f samples.

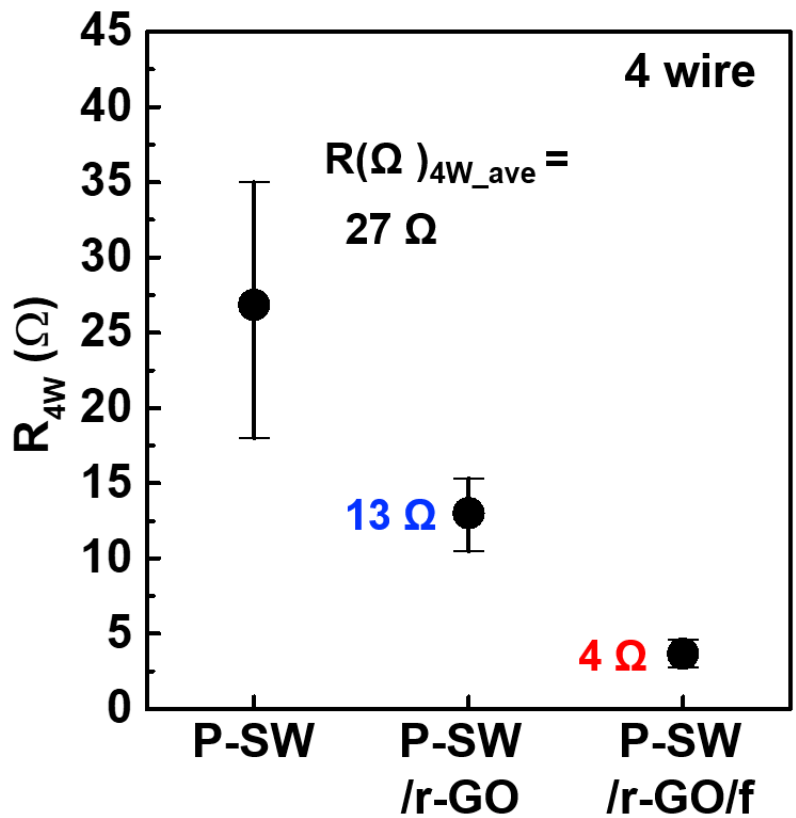


**Fig. S8** Electrical resistances of P-SW, P-SW/r-GO and P-SW/r-GO/f as conducting nanocomposite films by four-probe measurement.

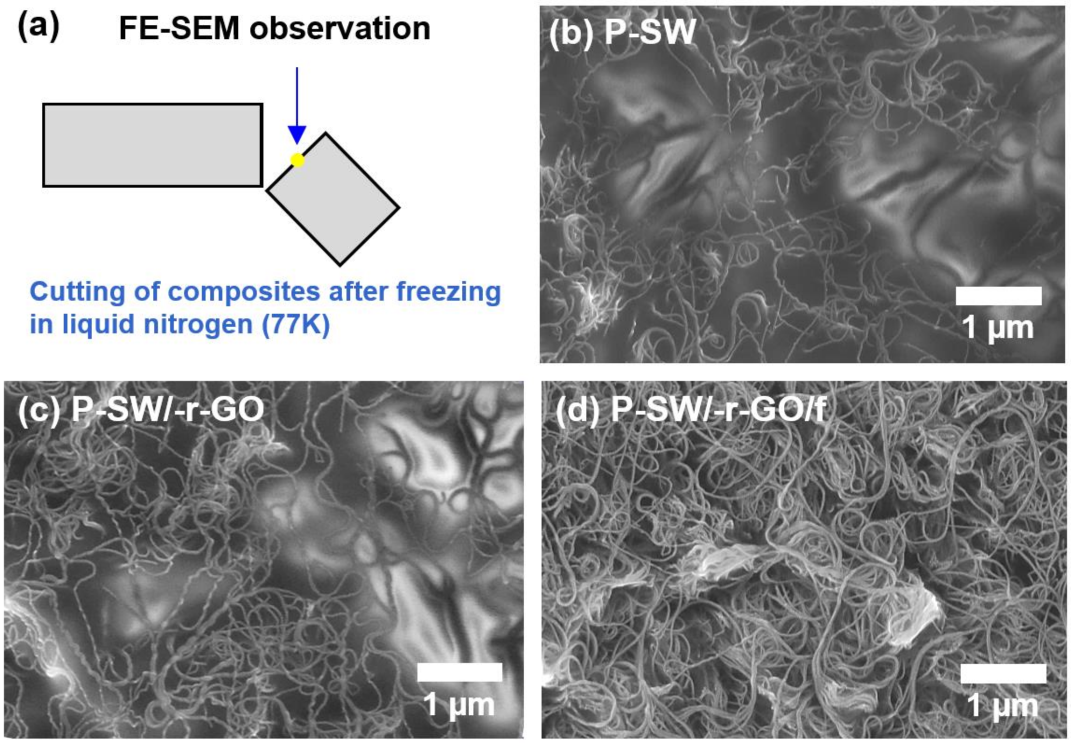


**Fig. S9** Cross-sectional FE-SEM images of the fabricated conducting nanocomposite films for (a) schematic of cutting composites, (b) P-SW, (c) P-SW/r-GO, and (d) P-SW/r-GO/f. Without charging, distinct cross-sectional images of P-SW/r-GO/f were observed via FE-SEM, owing to improved conductivity.

(a) (b)


**Fig. S10** Photographic images of the Movesense sensor (MODEL: OP174; diameter 36.6 mm & weight 9.4 g) (a) front and (b) back.

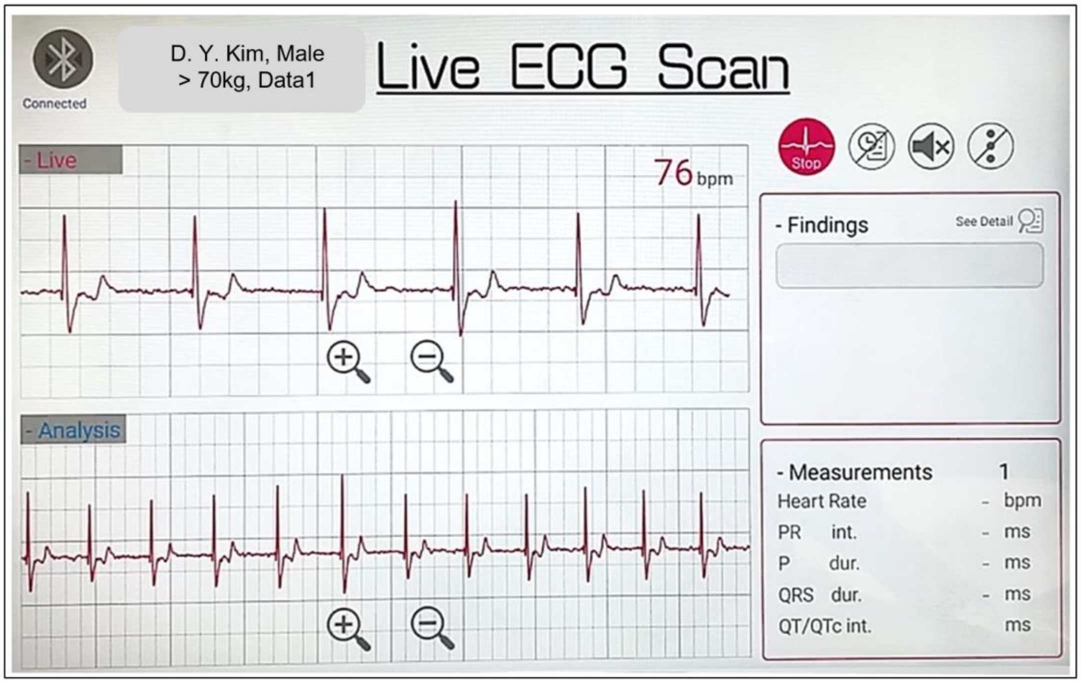


**Fig. S11** Self-developed tablet application for Bluetooth ECG monitoring.

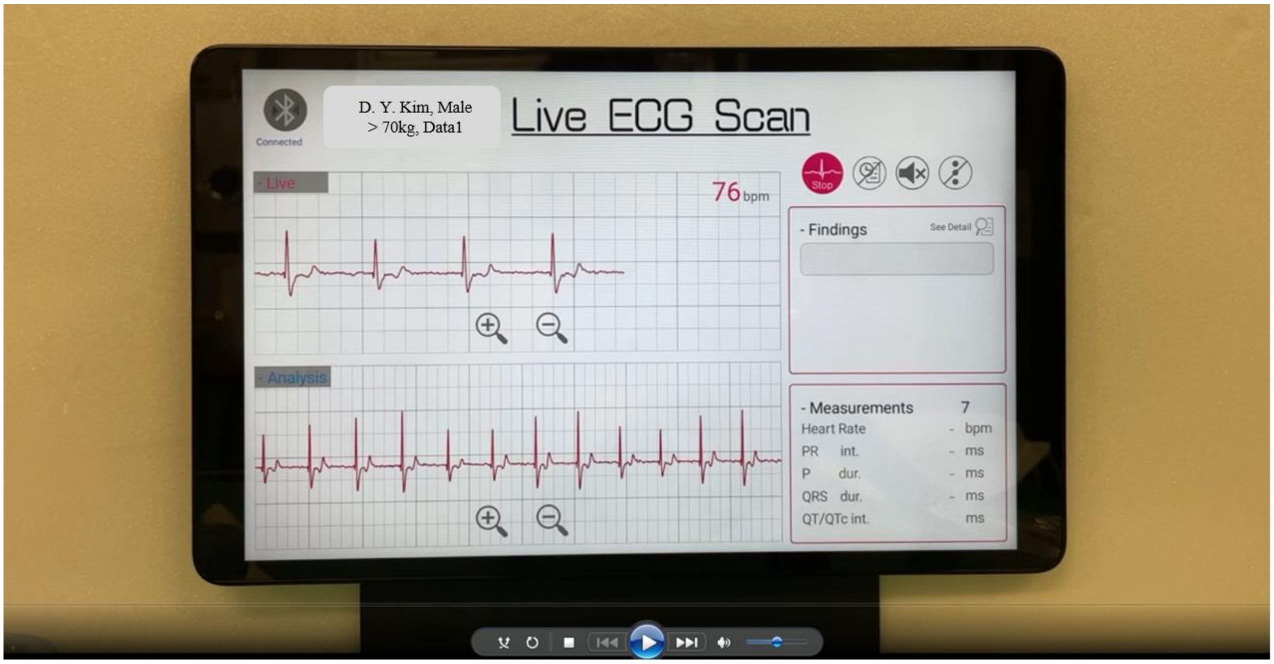


**Movie S1** Real-time measured ECG signal monitoring using self-developed tablet application.

**Table S4.** Comparison of the electrical properties of carbon nanomaterial-based composites.

| Carbon Materials | Conducting polymer | Material concentration | Electrical properties | Reference |
|---|---|---|---|---|
| SWCNTs | SWCNT/hydrogel structure | | 100–350 Ω/sq. | [1] |
| MWCNTs | Elastic CNT/PDMS composite | 1–20 wt.% | 2–7000 Ω/sq. | [2] |
| Graphene nanoplatelets | Screen printed graphene electrode on textile | - | 104 Ω/sq. | [3] |
| Graphene powder | Electronic tattoos based on silk and graphene | 40 wt.% | 96 ± 8 Ω/sq. | [4] |
| Graphene flakes | Electroconductive polymer spray-coated 3D porous graphene | - | 13–32 Ω/sq. | [5] |
| SWCNTs /r-GO | PDMS-based hybrid 1D SWCNTs/2D r-GO | SWCNTs (1 wt.%)/ r-GO (1 wt.%) | 4 Ω/sq. (at 4 wire) 15 Ω (at 2 wire) | This work |

[1] E. P. Gilshteyn, S. Lin, V. A. Kondrashov, D. S. Kopylova, A. P. Tsapenko, A. S. Anisimov, A. John Hart, X. Zhao and A. G. Nasibulin, *ACS Appl. Mater. Interfaces*, 2018, **10**, 28069–28075.

[2] J. H. Kim, J. Y. Hwang, H. R. Hwang, H. S. Kim, J. H. Lee, J. W. Seo, U. S. Shin and S. H. Lee, *Sci. Rep.*, 2018, **8**, 1375.

[3] X. Xu, M. Luo, P. He and J. Yang, *J. Phys. D Appl. Phys.* 2020, **53**, 125402.

[4] Q. Wang, S. Ling, X. Liang, H. Wang, H. Lu and Y. Zhang, *Adv. Funct. Mater.* 2019, **29**, 1808695.

[5] M. A. Zahed, P. S. Das, P. Maharjan, S. C. Barman, M. Sharifuzzaman, S. H. Yoon and J. Y. Park, *Carbon*, 2020, **15**, 26–36